J. Fluid Mech. (1988), *vol.* 188, *pp.* 185–204
Printed in Great Britain

On the entrainment rate across a density interface

By R. I. NOKES
Research School of Earth Sciences, Australian National University, Canberra, Australia

(Received 19 January 1987 and in revised form 4 August 1987)

Mixed-layer deepening due to grid-generated turbulence is studied experimentally with the aim of explaining the contradictory results of previous studies. Entrainment rates are calculated at fixed distances from the grid in order to avoid the necessity of using an empirical expression for the decay of the turbulent velocity scale. It is shown that an incorrect form of this decay law can cause large errors in the predicted Richardson number dependence of the entrainment rate. For this study this dependence can be expressed as a power law of the form $E = KRi^{-1.2}$. The spread of the results imply that an error of at least $\pm 10\%$ is realistic in the determination of the exponent.

The turbulent velocity decay law is also deduced from the data, and it is found that the decay cannot be represented by a simple power law. Indeed two distinct flow regions, with differing decay rates, are present.

1. Introduction

The occurrence of relatively sharp density interfaces in the natural environment (the thermocline in the ocean and inversions in the atmosphere are examples) has led to an interest in the characteristics of interfacial mixing. Much work, involving detailed laboratory experiments, has been aimed at improving the mixing models employed in these situations.

The system under consideration consists of two fluid layers, one of which is quiescent, while the other is stirred by turbulent motion (the mixed layer). Mixing between the layers is achieved principally through the activity of this turbulence, whose kinetic energy is transformed into a potential energy increase of the stratified system, or dissipated by friction. Some studies have concentrated on the turbulence generated by a mean shear, perhaps due to a wind stress on the surface of a large water body. A second line of research has focused on the turbulence generated with no mean shear present, and this has led to a long line of papers, beginning with Rouse & Dodu (1955) and Turner (1968), on grid-generated turbulence. Oscillating a horizontal grid some distance above or below a density interface has been seen as a convenient means of generating zero mean shear turbulence, with the essential properties of the turbulence, its length and velocity scales, determined by the grid geometry, the amplitude and frequency of oscillation and the distance from the grid. However, a number of questions regarding the mixing characteristics of this mechanically driven turbulence are still to be answered.

1.1. *Turbulence properties of an oscillating grid*

Too few studies have aimed directly at determining the turbulence characteristics of an oscillating grid. Fortunately, nearly all studies of this type have used the same grid as Turner (1968), or a scaled up version. Thompson (1969) analysed the

turbulence created by oscillating grids and bars of various geometries. His results, published later in Thompson & Turner (1975), demonstrated that for Turner's square-barred grid, the turbulent lengthscale, taken to be the integral lengthscale, increased linearly with distance from the grid, while the velocity scale, taken to be the root-mean-square of the horizontal velocity fluctuations, decayed with distance from the grid to the power of 1.5. Their results also showed that the velocity scale was proportional to the frequency of oscillation.

Hopfinger & Toly (1976) reported a comprehensive study of the turbulence properties of two grids, similar to that of Turner (1968). They confirmed the linear dependence of the lengthscale of the turbulent motions on the distance from the grid, measured from a virtual origin. The determination of this virtual origin is an important element in studies of this type. Power-law exponents are known to be sensitive to errors in this parameter, and its selection, therefore, must be made in a way consistent with other studies. The method chosen by Hopfinger & Toly seems least ambiguous. They defined the virtual origin as the height in the fluid at which the integral lengthscale became zero. This point was found to lie slightly behind the grid midplane in its equilibrium position. Their results also demonstrated that the constant of proportionality relating the lengthscale to the distance from the grid was both stroke and mesh dependent. Their detailed velocity measurements allowed them to deduce an empirical relation for the turbulent velocities, depending on the frequency and amplitude of oscillation, mesh size and distance from the grid. It is given by

$$u = 0.25 f S^{1.5} M^{0.5} z^{-1}, \tag{1}$$

where u is the turbulent velocity scale, f the frequency, S the stroke, M the mesh size (i.e. distance between bar centres), and z the distance from a virtual origin. The exponent of the velocity decay exhibited some spread, and, for small stroke to mesh ratios, an exponent of -1.25 seemed to be a better fit to the data. Uncertainties in the position of the virtual origin were estimated to cause an error in the exponent of $\pm 4\%$. The decay of the velocity scale ($u \propto z^{-1}$) was found to be less rapid than that quoted by Thompson & Turner (1975). In fact, Hopfinger & Toly demonstrated that Thompson & Turner's data, for a square-barred grid, were more accurately represented by a z^{-1} law than a $z^{-1.5}$ relation.

McDougall (1979) made careful measurements of the flow generated by Turner's grid and showed that the turbulence is far from homogeneous in the horizontal, even 10 cm away from the grid (his stroke was 1 cm). His results also demonstrated that an upper frequency limit existed, above which the turbulent velocity scale was no longer linearly related to frequency. This cutoff occurred at approximately 7 Hz.

More recently, Hannoun, Fernando & List (1988) have reported a comprehensive study of the effect a density interface or rigid boundary has on the turbulence generated by an oscillating grid. Using laser-induced fluorescence techniques to measure the motions of the interface, and a two-component laser-Doppler velocimeter to monitor the turbulent velocities, they were able to deduce energy spectra, velocity correlations and kinetic energy fluxes, as well as turbulent intensities. Their results demonstrated that the large-scale turbulent eddies are flattened in the vicinity of either a rigid boundary or density interface, and energy is transferred from the vertical turbulent motions to the horizontal. As the grid used by Hannoun *et al.* (1988) had a different geometry to the square-barred grid employed by previous investigators, care should be taken in comparing the measured turbulence characteristics.

Long (1978) published a theoretical model of the turbulence field generated by an

oscillating grid in a homogeneous fluid. This model predicts that the turbulence may be characterized as a single quantity called 'grid action', proportional to the product of the turbulent lengthscales and velocity scales, and therefore representing some form of turbulent diffusivity. The results of Dickinson & Long (1978, 1983) lend support to the concept of grid action, and confirm the theoretical prediction that the turbulent layer, in a homogeneous fluid, grows as the square root of time.

1.2. *Entrainment across a density interface and its Richardson number dependence*

In addition to these studies, much work has concentrated on the entrainment rate across a density interface, and its dependence on a Richardson number, based on the turbulence properties at the position of the interface, if the interface were not present. The Richardson number represents a measure of the relative importance of buoyancy to inertial forces (implicitly assuming that viscosity plays no role in the mixing process), and is defined by $Ri = g\Delta\rho l/\rho u^2$ where g is the gravitational acceleration, $\Delta\rho$ the density jump across the interface, l the turbulent integral lengthscale, and ρ the density of the mixed layer. Systems have been studied where the quiescent layer is either homogeneous or linearly stratified. Details of these studies can be found in Turner (1968), Linden (1975), Wolanski & Brush (1975), Hopfinger & Toly (1976), McDougall (1978), Folse, Cox & Schexnayder (1981), Fernando & Long (1983, 1985), E & Hopfinger (1986) and Hannoun & List (1988).

Despite this concentrated experimental effort, no consensus has been reached on a universal relationship between the Richardson number and the entrainment velocity, u_e, defined as the rate at which the interface between the two layers advances into the quiescent layer. There are three conflicting hypotheses. The first favours a power-law dependence of the following form:

$$E = KRi^{-1.75}, \tag{2}$$

where E is the ratio of the entrainment velocity to the turbulent velocity scale, and K is constant. The work of Fernando & Long (1983, 1985) offers convincing verification of this relationship, while the results of Folse *et al.* (1981) also give moderate support to its validity. However, this latter study considered the mixing due to a finely woven mesh, not a grid.

The second group proposes a relationship of the form:

$$E = KRi^{-1.5}. \tag{3}$$

This particular relation is strongly supported by the results of E & Hopfinger (1986), and Wolanski & Brush (1975), and to a lesser extent by the work of Turner (1968) and Hopfinger & Toly (1976). The results of the two latter studies yield exponents only approximately equal to -1.5, although they are certainly closer to this value than to -1.75. Turner found that the entrainment rate was the same, whether one or both of the two fluid layers were stirred. This important observation lends strong support to the proposition that mixing at the interface takes place intermittently, and rarely enough for the mixing events on each side of the interface to be treated independently. Hannoun & List (1988) also support (3), although for practical reasons they were only able to cover half an order of magnitude variation in Richardson number.

Finally, McDougall (1978) presents experimental evidence that suggests that the magnitude of the exponent in (3) is considerably less than 1.5. In fact, he deduces an

exponent of -1.08. In support of this result he demonstrates that a best fit to Turner's (1968) results, for $Ri > 5$, yields an exponent of -1.31, not -1.5 as is commonly quoted. In conclusion, he suggests that a value of -1.2 ± 0.12 may be a better estimate of the exponent.

It is the misfortune of the modeller wishing to choose between these three expressions, that the first two entrainment relations have theoretical support. Long (1978) has presented a complicated theory of the mixing process in a stratified system, based on the concept of the intermittent breaking of internal waves in the interfacial region between the mixed and quiescent layers, which predicts the entrainment relation expressed in (2). In contrast, Linden (1973) has suggested a simple model in which the mixing takes place during the recoil of the interface, following its interaction with a turbulent eddy. To support his theory, Linden conducted some elegant experiments in which vortex rings, intended to simulate turbulent eddies, collided with a density interface. His calculations support the second entrainment law given in (3). E & Hopfinger (1986) point out that it is somewhat surprising that these two theories, both of which contend that the mixing is controlled by the buoyancy timescale of the disturbed interface, and not the eddy overturn timescale, do not yield identical results. Recently Hannoun & List (1988) have proposed a theory similar to that of Long, based on an oceanic mixing model of Phillips (1977). While the concept of local internal wave breakdown is also central to their model, detailed differences between their theory and Long's (the dependence of the wave velocities and interfacial thickness on Richardson number) result in their model supporting (3).

Further work is needed if the cause of the discrepancy between these three entrainment laws is to be resolved. This study sets out to achieve this aim, and comparison will be made continually with the results of Fernando & Long, and E & Hopfinger, as the two principal proponents of the first two power laws, and McDougall. Perhaps the only conclusion that can be drawn from the completed work in this field, is that grid-generated turbulence and its use as a tool in mixing studies is considerably more complex than might be expected.

In the future is is likely that more sophisticated experimental techniques, such as those used by Hannoun and his collaborators, will be needed to resolve the issue. However it appears that more information can still be gained from simple experiments of the type used in the majority of previous studies. At a fixed distance from the grid the turbulent velocity scale and lengthscale are constant, if unknown. Measurements of the entrainment rate as a function of the density difference between the layers then will yield the required entrainment law to within a numerical constant. This technique reduces the need for direct turbulence measurements. This is the approach first used by Turner (1968), although his main interest was the influence of molecular processes on the entrainment rate, and he did not vary the distance from the grid at which his measurements were made nor did he vary the stroke. If an assumption regarding the growth of the turbulent lengthscale is made then the technique employed in this study also allows the decay rate of the velocity scale to be deduced.

Section 2 describes the experimental apparatus and procedures used in the present study, and includes an outline of the data analysis method. The experimental results are presented in §3 where the deduced entrainment and velocity decay laws are discussed. Also included in this section is a brief discussion of the effect of having the grid placed near a solid boundary. Finally §4 summarizes the results and attempts to use the conclusions reached to understand the discrepancy in previously published results.

2. Experimental apparatus and procedures

Figure 1 shows a schematic representation of the experimental configuration. The Perspex experimental tank was 25.4 cm square, and 60 cm deep. It therefore had the same horizontal cross-section as the tank used by Turner (1968). The grid was also identical to Turner's, with 1 cm square bars at 5 cm centres. The grid was positioned in the bottom layer of fluid, and driven from below by a Scotch yoke attached to a small electric motor, whose speed of rotation was monitored by a photoelectric cell. Both the stroke, and the grid's position above the bottom of the tank were adjustable.

Common salt was always the stratifying agent, with red food dye occasionally added to the bottom layer for visual effect.

The depth of the mixed layer was determined by measuring the density of the bottom-layer fluid as top-layer fluid was entrained across the interface. Other experimenters have calculated the depth from shadowgraph records of the motion in the tank, but this is particularly difficult when the interface is very active. Bottom-layer fluid was withdrawn from the flow through a stainless steel probe, of 1.2 mm inside diameter, by the action of a peristaltic pump. The fluid passed through an Anton Parr density meter and returned to the tank via another length of hyperdermic tubing. The two probes were always placed slightly above the highest position reached by the grid. A flow rate of less than 6 ml/min was required to ensure that the density measurement was accurate, and this guaranteed that the withdrawal of fluid had no effect on the flow, except in the vicinity of the probe.

The voltage output from the density meter was logged continually by a microcomputer, giving a continuous record of density against time. All of the subsequent analysis of the data was performed on the microcomputer, or by hand.

The measured densities were converted to salt concentrations from standard tables (Weast 1984). If the interfacial layer thickness h, is assumed to be negligibly small, the mixed-layer depth (the mixing process is assumed to be one-dimensional and therefore the mixed-layer depth represents a spatial average) may be deduced from the conservation of salt in the bottom layer. Thus

$$D' = \frac{B}{c_s} - z_0, \tag{4}$$

where B is the product of the initial salt concentration and height of the interface above the tank bottom, c_s is the salt concentration in the bottom layer, and D' and z_0 are defined in figure 1. The entrainment velocity u_e is therefore given by $\mathrm{d}D'/\mathrm{d}t$.

The derivative, $\mathrm{d}D'/\mathrm{d}t$, was calculated in two ways. Firstly, a smooth curve was drawn through the function $D' = D'(t)$ and a derivative was calculated by constructing a tangent to the line. Secondly, the derivative was calculated as a function of time on the microcomputer using linear interpolation between adjacent points. (Note that in a typical experimental run between 1000 and 2000 density measurements were taken.) These two methods generally gave values for u_e to better than 10% accuracy. Only for small Richardson numbers, when entrainment was rapid, were the derivative estimates less reliable than this and generally these results were not retained for future analysis.

Other studies have suggested that the interfacial layer is not negligibly thin. The work of Crapper & Linden (1974) and Fernando & Long (1985) showed that h/D (both h and D are defined in figure 1) is constant, with a value of approximately 0.1.

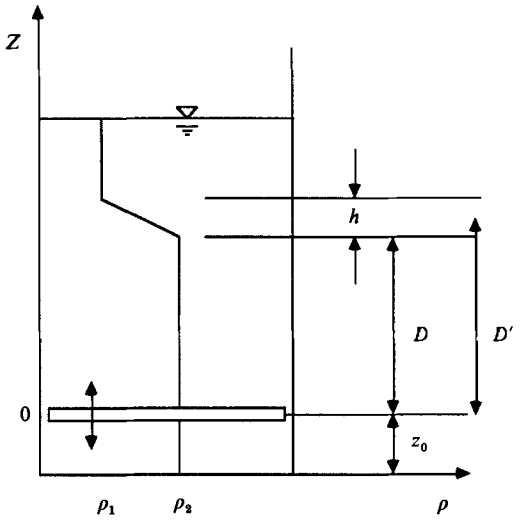

FIGURE 1. The experimental configuration represented in schematic form.

In contrast, E & Hopfinger (1986) found h/D to be Richardson number dependent, taking a value of about 0.06 for very large values of Ri, and increasing as Ri decreased. Further debate has been fuelled by the results of Hannoun & List (1988) that show h/D decreasing with Richardson number, from a value of about 0.014 at $Ri = 25$ down to values as small as 0.003 for a Richardson number of about 100. For interfaces this thin, molecular transport will become important.

These contrasting results leave the effect of assuming a negligibly thin interfacial layer rather uncertain. If the results of Hannoun & List are correct then this approximation will lead to accurate estimates of the true entrainment velocity, at least over the range of Richardson numbers covered in their experiments. On the other hand, if the interface is a finite but constant proportion of the mixed-layer depth then the ratio of $\mathrm{d}D'/\mathrm{d}t$ to $\mathrm{d}D/\mathrm{d}t$ will be constant and the use of $\mathrm{d}D'/\mathrm{d}t$ will not effect the functional form of the deduced entrainment law. Only if the thickness of the interface changes significantly with Richardson number will errors arise in the deduced form of the entrainment relation. Throughout this study $\mathrm{d}D'/\mathrm{d}t$ is used to calculate the entrainment velocity but the consequences of D/D' being Richardson number dependent will be discussed in §3.1.

As mentioned in the introduction the principal difference between the present study and the major studies of E & Hopfinger (1986), and Fernando & Long (1983, 1985) is the method of analysing the data. By measuring the entrainment at a fixed distance from the grid there is no need to resort to empirical expressions for the velocity scales and lengthscales of the turbulent motions. Turner (1968) used the same technique, withdrawing fluid from the bottom layer in order to keep the interface at a fixed level. In this study the interface is allowed to move away from the grid, and a number of runs, with varying initial density differences, are made with the same amplitude and frequency of oscillation. The entrainment rates for one particular mixed-layer depth can then be collated from all runs, and an entrainment relation deduced (see §2.1).

The turbulent velocity decay is of paramount importance in determining the functional form of the entrainment velocity's dependence on Richardson number. If E is assumed to be proportional to $Ri^{-1.5}$ then $u_e \propto u^4$, while $u_e \propto u^{4.5}$ if $E \propto Ri^{-1.75}$.

A small error in the assumed form of $u(z)$ will cause a significant error in the deduced entrainment law. This will be clearly demonstrated in §3.2.

The velocity decay law also may be found from the method of analysing the data, described above. By collapsing the entrainment relations obtained for a number of mixed-layer depths, the variation of the turbulent velocity with distance from the grid is obtained (see §2.1), provided the growth rate of the turbulent lengthscale with distance from the grid is assumed.

The frequency of oscillation was set at 4 Hz for all runs. It is generally acknowledged that the velocity scale is linearly proportional to frequency, as any other relationship would demand, for dimensional reasons, the appearance of the viscosity in the expression for velocity. Therefore, there seemed little point in varying this parameter. However, the stroke was varied, taking five different values between a minimum of 0.77 cm, and a maximum of 4.9 cm.

The effect of varying the distance from the grid to the bottom of the tank, z_0, was also briefly investigated. It was hoped that this would offer some insight into the manner in which the presence of a solid boundary affects the distribution of turbulent kinetic energy in the tank.

The turbulent motions in a homogeneous fluid were observed by seeding the fluid with neutrally buoyant fish scales and illuminating the tank from both sides through vertical 1 cm wide slits. When the fluid is quiescent the light reflected by the scales is of uniform intensity. Turbulent motion is identified by the appearance of light and dark patches in the fluid.

2.1. *Data analysis*

The extraction of the important experimental results from the experimental data is briefly discussed in this section. While no fundamental reason exists for a power dependence of the entrainment velocity on Richardson number, the experimental evidence published so far strongly supports this relationship, provided Ri is not too small. Therefore the entrainment law may be written as

$$\frac{u_e}{u} = K\left[\frac{g\Delta\rho l}{\rho u^2}\right]^{-n}. \tag{5}$$

Again, purely empirical evidence suggests that the turbulent lengthscale is linearly related to the distance from the grid and that the velocity decay law may be well represented by a power law relation. Thus

$$l = \beta z, \tag{6}$$

$$u = AfS\left[\frac{z}{Z}\right]^{-\alpha}, \tag{7}$$

where A, β and Z do not depend on z. A is dimensionless, and may be a function of the ratios of the various lengthscales in the system, the stroke, mesh size and bar thickness. It may be Reynolds number dependent also, although this would require an f/ν (where ν is the kinematic viscosity) dependence. As a result u is no longer proportional to f to the first power, in disagreement with the results of McDougall (1979) and Thompson & Turner (1975) for the same grid. The Reynolds numbers of our flows were generally larger than those of McDougall and Thompson & Turner and therefore an Re dependence is unlikely. Even so, if A is Re dependent, provided this dependence can be expressed as a power law the form of the z-dependence in (7) is unchanged.

β, which is dimensionless, and Z, which has the dimensions of length, may depend on the same three lengthscales as A. A linear relation between the lengthscale of the turbulence and the distance from the grid, measured from a virtual origin (taken to be the middle of the grid in its equilibrium position), is widely accepted. Thompson & Turner (1975) give 0.1 as the constant of proportionality, and this seems valid for small strokes. The results of Hopfinger & Toly (1976) suggest that this constant is dependent on the stroke and mesh size. For the results presented here, $l = 0.1D'$ is used for all strokes. This assumption has no effect on the deduced forms of the entrainment law or velocity decay law, as the results for each stroke are considered separately. However, if the velocity dependence on stroke is to be deduced from the present measurements (see §3.4) the stroke dependence of β must be known.

If the product $fS = u_0$ is used as the velocity scale at all levels in the flow, then the entrainment relation may be expressed as

$$E^* = \frac{u_e}{u_0} = CRi^{*-n}\left[\frac{z}{Z}\right]^{-\gamma}, \tag{8}$$

where $\gamma = \alpha(1+2n)$, $Ri^* = (\Delta\rho g l/\rho u_0^2)$ and C is a constant depending upon A and K. Taking the logarithm of equation (8) yields:

$$\ln E^* = \ln C - n \ln Ri^* - \gamma \ln\left[\frac{z}{Z}\right]. \tag{9}$$

When $\ln E^*$ is plotted against $\ln Ri^*$ (Ri^* is calculated with $l = 0.1z$ for all strokes) a series of straight lines will be obtained, corresponding to the entrainment relations for each mixed-layer depth. The slope of each line yields an estimate of the exponent, n. For one particular stroke the value of Z is fixed. Therefore, the value of γ may be obtained by calculating the x-axis translation required to collapse all of the entrainment curves onto a single line. Thus

$$\ln E^* = \ln C' - n \ln Ri^{*\prime}, \tag{10}$$

where

$$\ln Ri^{*\prime} = \ln Ri^* + \frac{\gamma}{n} \ln\left[\frac{z}{z^*}\right]. \tag{11}$$

C' is a constant depending on C and Z, and z^* is the mixed-layer depth corresponding to the reference line on to which all the other curves have been collapsed. If the x-axis translation is designated $f(z)$, then the velocity decay power, α, is calculated from the slope of a plot of $nf(z)/(2n+1)$ against $\ln(z/z^*)$.

It has been noted in the introduction that all distances from the grid are measured relative to a virtual origin. While it is true that the resulting power law exponents are quite sensitive to the choice of virtual origin, a number of studies have found that it is very close to the midplane of the grid in its equilibrium position, that is, halfway between the two extreme positions of its motion. The calculations described in this paper abide by this convention.

Run number	Stroke (cm)	$\Delta\rho_0$	z_0 (cm)	Range of D' (cm)	n
NV2	3.22	0.022	7.5	11–15	1.26
NV3	1.6	0.0069	7.5	6–11	1.26
NV4	1.6	0.012	7.5	6–11	1.22
NV5	1.6	0.0032	7.5	7.5–11	1.43
NV6	1.6	0.024	7.5	6–10	1.11
NV7	1.6	0.045	7.5	6–10	1.08
NV8	1.6	0.0050	7.5	7–10	1.35
NV9	1.6	0.0013	7.5	9.5–11	—
NV10	2.4	0.0094	11.25	8–11	1.61
NV11	2.4	0.038	11.25	6–11	1.22
NV12	2.4	0.075	11.25	6–10	1.12
NV13	2.4	0.020	11.25	7–11	1.37
NV14	2.4	0.113	11.25	6–9.5	1.06
NV16	0.77	0.0031	3.84	6–10	1.17
NV17	0.77	0.0011	3.84	6.5–10	1.18
NV18	0.77	0.0023	7.55	6–10	1.21
NV19	3.22	0.051	11.12	7.5–15	1.25
NV20	3.22	0.011	11.12	9–15	1.22
NV21	3.22	0.097	11.12	7.5–15	1.21
NV22	4.9	0.052	19.55	12–22	1.25
NV23	4.9	0.081	19.55	12–22	1.42
NV24	4.9	0.144	19.55	12–22	1.36

TABLE 1. The experimental data for all runs

3. Results

Table 1 lists the experimental parameters for each run.

3.1. *Entrainment relation*

The results for a stroke of 1.6 cm (runs NV3–NV9) are presented in figure 2. E^* is plotted against Ri^* on log–log paper and a series of lines is obtained, corresponding to the entrainment relations at various distances from the grid. For each mixed-layer depth, the straight lines on the log–log plot were calculated by a least squares best fit to the data. The exponent of the power law relation between the non-dimensional entrainment velocity, and the Richardson number is calculated from the slope of each of the lines drawn. Figure 3 presents the values of n as a function of distance from the grid, deduced from the results for all strokes.

For practical reasons, only for strokes of 1.6, 2.4 and 3.22 cm was it possible to cover an order of magnitude or more variation in Richardson number. The results for these three strokes yield mean values of the exponent, n, of 1.18, 1.22 and 1.23 respectively. The line marked Nokes in figure 3 represents an average of these values. Clearly, while these results are internally consistent, the predicted reduction in entrainment rate with Richardson number fails to agree with either the results of E & Hopfinger, or Fernando & Long, although it is in agreement with the suggestion of McDougall.

There is considerable scatter in the values of n obtained for each mixed-layer depth. Combining the results for these three strokes, n is found to vary between 1.04 and 1.31. This spread does not appear to be entirely random, as would be expected

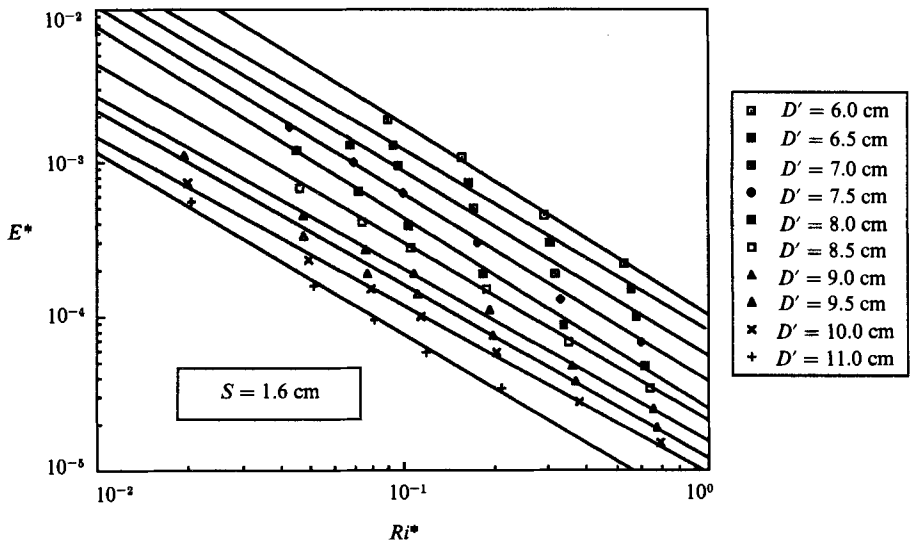

FIGURE 2. For a stroke of 1.6 cm (runs NV3–NV9) the entrainment relations for various distances from the grid are presented. The lines represent least squares best fits to the results at each height. Their slopes are given in figure 3. Both E^* and Ri^* have been non-dimensionalized by the velocity u_0.

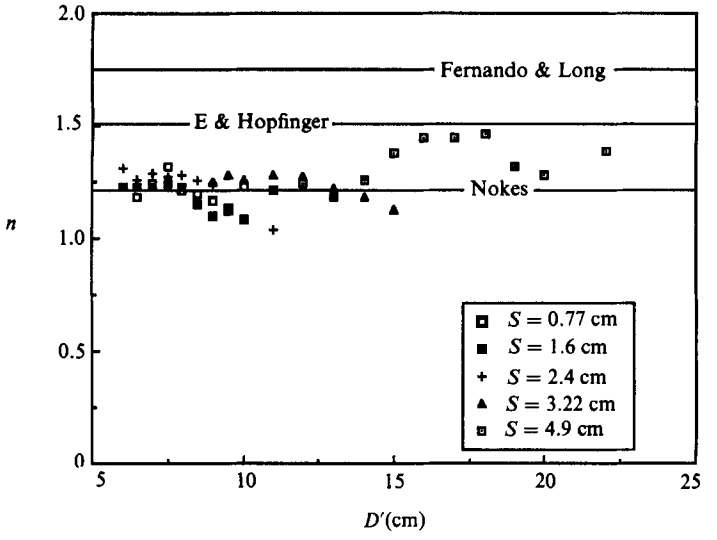

FIGURE 3. The exponent of the entrainment relation, n, given as a function of mixed-layer depth. The results for all strokes are included, and the predictions of E & Hopfinger (1986) and Fernando & Long (1983, 1985) are also illustrated.

if it were due solely to experimental scatter. The results for each stroke show a tendency for n to decrease as the mixed-layer depth increases, the result for $S = 1.6$ cm and $D' = 11.0$ cm being the exception. A possible explanation for this is that the relationship between E and Ri is not an exact power law, and that a plot of E against Ri on a log–log plot will yield a line with some curvature. To be consistent with the falloff of n with increasing D', the slope of this curve would need to be less negative for greater values of Ri. It will be seen that when all of the results are collapsed onto

one entrainment curve, the experimental scatter smothers any sign of this curvature. The presence of significant molecular transport at high Richardson numbers, as suggested by the results of Hannoun & List (1988), is another possible reason why the value of n becomes less negative as Ri increases.

The results for strokes of 0.77 and 4.0 cm are also presented in figure 3. For these two strokes a variation in Ri of only about a factor of 3 could be obtained. Because of this, the slopes of the curves on a log–log plot were poorly constrained, and the calculated values of n less reliable. It can be seen in figure 3 that the results for the small stroke are consistent with the results already discussed (mean value of $n = 1.22$), while those for the largest stroke exhibit considerable scatter with a mean value of 1.34.

The results presented in figure 3 would suggest that the error in determining the correct value of n is at least $\pm 10\%$.

We now return to a point discussed briefly in §2. By assuming that the interfacial-layer thickness is a constant proportion of the mixed-layer depth, D is always a fixed fraction of D', and the calculated entrainment velocity is proportional to the true value of u_e. However, if the results of E & Hopfinger (1986) are correct, D/D' varies with Richardson number, decreasing as Ri decreases. When considered in the light of the present method of analysis, the effect of this is twofold. Firstly, the entrainment velocity for small Richardson numbers is overestimated by the present analysis. As a consequence, the lines plotted in figure 2 have their slopes increased. Secondly, the lines in figure 2 no longer correspond to constant values of D. Instead, the value of D for small Richardson numbers is less than that for larger values, and the slope of a line of constant D will be greater than that of a line of constant D'. Both effects result in a smaller value of n than that given by assuming D/D' is constant. It is important to recognize that a Richardson number dependence of D/D' does not help, in any way, to reconcile the results of the present study with those of E & Hopfinger, and Fernando & Long. Rough calculations, using the results of E & Hopfinger as a guide, suggest that n may be overestimated by about 10% by assuming that D/D' is independent of Ri.

A comparison with the results of Turner (1968) is essential, as his experimental configuration was, in essence, the same as that described in §2, and, in addition, his entrainment relation was deduced from measurement at a fixed distance from the grid. While the value of n deduced from his measurements is quoted as 1.5, a least squares best fit demonstrates that it is significantly less, as was first recognized by McDougall (1978). Using the data points with a Richardson number greater than 5 (see figure 9.3 Turner 1973), yields a value of n equal to 1.34. This difference can be seen in E & Hopfinger's (1986) figure 4(*a*), where Turner's data are compared with their own, and the two data sets have different slopes.

Turner's results should agree with the conclusions of this study, because of the close similarity in the experimental configurations and analysis methods. His data do exhibit more scatter than the results of this study, and thus may be less precise. However, the discrepancy offers further insight into the accuracy to which the exponent of the entrainment relation can be deduced from experiments of this kind. An error of $\pm 10\%$ in calculating the exponent, as suggested above, is probably a lower bound.

3.2. *Velocity decay law*

The curves drawn in figure 2 all correspond to the same entrainment law. Only the relative turbulent velocities at each distance from the grid are unknown. As

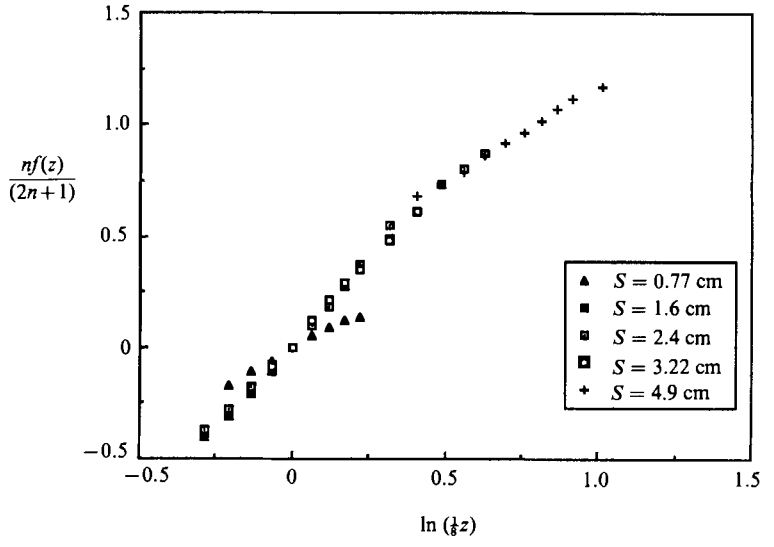

FIGURE 4. The entrainment curves (like those in figure 2) are collapsed onto the $D' = 8$ cm curve by a translation in the x-direction, $f(z)$. $nf(z)/(2n+1)$ is plotted against non-dimensional distance from the grid. The slope of the data is α, the negative of the velocity decay law exponent.

demonstrated in §2.1, the velocity decay with z may be calculated by collapsing these curves onto a single line. The curve for $D' = 8$ cm was taken as the reference line (z^*) in all cases except for $S = 4.9$ cm, when $D' = 15$ cm was selected. The function $nf(z)/(2n+1)$, defined in §2.1, is plotted against $\ln(\frac{1}{8}z)$ in figure 4. As the slopes of the curves in figure 2 vary somewhat, the translation in the x-direction, necessary to collapse the data, was determined by eye.

For strokes of 1.6, 2.4 and 3.22 cm the results are consistent with a decay law of $z^{-1.5}$, valid for $6 < D' < 12$ cm. The actual slopes for these three strokes are 1.52, 1.51 and 1.46. At a distance of approximately 12 or 13 cm the results for $S = 3.22$ cm show a marked decrease in the slope of the data, although more results further from the grid would be needed to determine accurately its new value.

The results for the largest stroke, 4.9 cm, which have been presented in figure 4 by equating the value of $nf(z)/(2n+1)$ at $z = 13$ cm with that for a stroke of 3.22 cm, show a velocity decay of the form $z^{-0.86}$. This apparent change in the decay law implies that a universal power law, as suggested by Hopfinger & Toly (1976), may not be valid. The decay of velocity for a 0.77 cm stroke has a form close to that of the largest stroke, namely $z^{-0.8}$, although in this case the power law is valid between $D' = 6$ cm and $D' = 10$ cm.

In an attempt to ascertain, at least qualitatively, a reason for the existence of a number of velocity decay laws, apparently stroke- and z-dependent, the turbulent motions generated by the grid in a homogeneous fluid were observed by seeding the flow with neutrally buoyant, microscopic fish scales. The resulting turbulent motions are identified by light and dark patches in the flow when the tank is illuminated through 1 cm slits on each side of the tank. Figure 5 illustrates the observed motion for a stroke of 2.4 cm and a frequency of 4 Hz.

Two distinct regions exist. The first, near the grid, is quite coherent, and appears to have the form of a number of turbulent wakes. Beyond this region, and separated from it by an ill-defined boundary, is a zone of incoherent turbulent motions with

FIGURE 5. The turbulent motions generated by the grid, with a 2.4 cm stroke and frequency of 4 Hz, in a homogeneous fluid seeded with fish scales and illuminated through 1 cm wide slits. Regions of strong turbulent activity, in the form of turbulent wakes, can be seen near the grid, extending approximately 10 cm from the virtual origin. The divisions on the left of the photograph are at 1 cm intervals. The bottom arrow on the left of the photograph marks the grid's mean position and the top arrow identifies its position at the top of its stroke. The photograph was taken with a 1 second exposure.

apparently no mean horizontal structure, extending to the top of the tank. The approximate position of the boundary between these two flow regions was estimated from observations of the flow field. For strokes of 1.6, 2.4 and 3.22 cm this boundary was located approximately 10–13 cm from the grid midplane, apparently independent of the stroke. Because of the considerably more vigorous motions associated with a stroke of 4.9 cm, the limit of the coherent zone was difficult to determine. However, it was estimated to be, if anything, a little closer to the grid than that for the three smaller strokes. Finally, with the smallest stroke, $S = 0.77$ cm, the zone nearest the grid was found to extend barely 3 or 4 cm from the grid midplane.

A number of tentative conclusions may be drawn from these qualitative results. Firstly, two distinct regions appear to exist in the turbulent flow field. Near the grid the turbulence exhibits a definite horizontal structure, while further from the grid the turbulent motions have little or no mean horizontal variation. The transition between these zones appears to be relatively rapid, and for strokes larger than the bar size, the transition level is between 10 and 13 cm from the virtual origin, and essentially independent of stroke. Secondly, these observations are supported by the deduced velocity decay which demonstrates a definite change in the decay law approximately 12 cm from the grid midplane. The results presented in figure 4 also show that, provided the stroke is greater than the bar size, the velocity decay law has a z-dependence independent of stroke. Thus it may be concluded that Z, defined in equation (7), depends only on the grid geometry. Finally, the observations predict that the velocity decay between $z = 6$ and $z = 10$ cm, for the smallest stroke, should be like that in the incoherent region. This is in fact the case. The data for $S = 0.77$ cm, presented in figure 4, show a gradual decay of velocity with z, with a slope of approximately 0.8.

The changing form of the turbulent flow structure causes some concern with regard to the mixing results when it is remembered that horizontal homogeneity has been implicitly assumed. It would be expected that the mixing characteristics of the two flow regions would be quite different, and that only the results obtained outside the zone characterized by the coherent wake structures would be meaningful. However the results of this study (see figure 3) strongly support the conclusion that the rate of interfacial mixing has the same Richardson number dependence whether or not the turbulence is laterally completely homogeneous, provided that representative velocity and lengthscales are used to specify the turbulent motions. Certainly the results for the smallest stroke, all of which were obtained in the absence of the wake structures, yield the same Richardson number dependence as the results with the larger strokes, which were obtained within the laterally heterogeneous region.

The entrainment curves for each stroke were collapsed onto one curve using the deduced velocity decay law. Figure 6 shows the results for strokes of 1.6 and 3.22 cm ($\hat{E}$ and $\hat{R}i$ are defined such that the turbulent velocity scale is equal to u_0 at $z = 8$ cm and the velocities at other levels in the flow are calculated relative to this value using the deduced velocity decay law). In all cases no more than a 1% difference was found between the slope of the combined curve, and the average slope of the curves for different mixed-layer depths. The entrainment results for each experimental run were rescaled with the deduced velocity decay law, resulting in a value of n being calculated for each run. These values are listed in table 1. A considerable spread is obtained, with all of the results except one (NV10) lying within the limits $1.06 \leqslant n \leqslant 1.43$. The trend referred to in §3.1 is again identifiable, with the

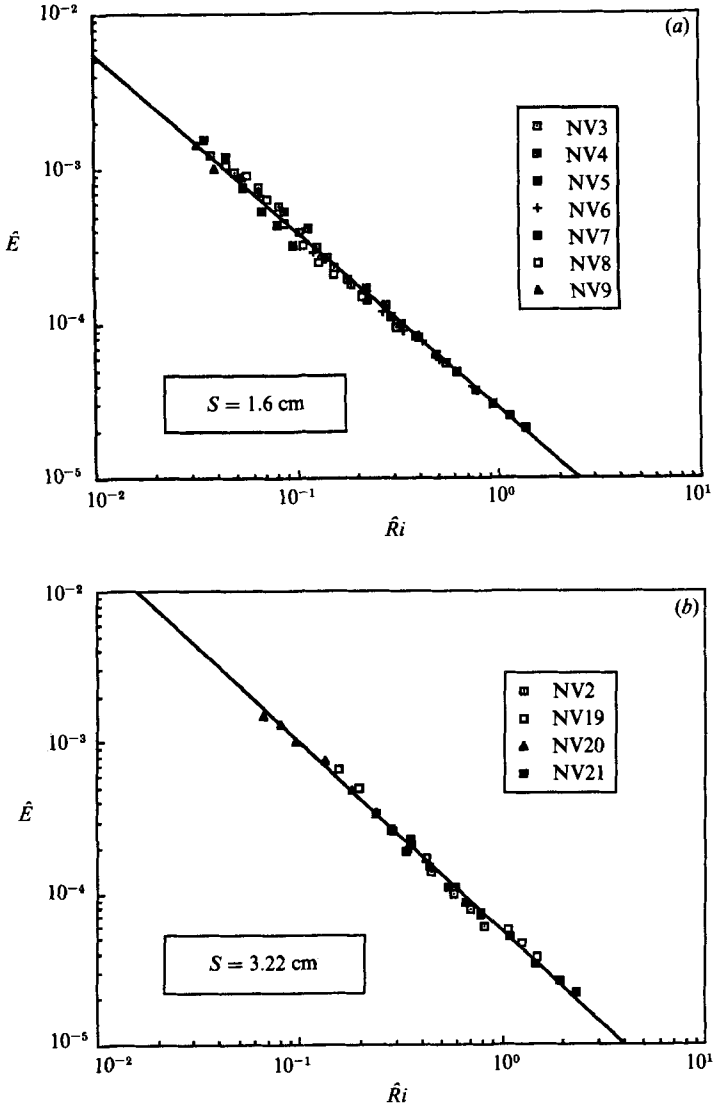

FIGURE 6. (*a*) The entrainment relation obtained for a stroke of 1.6 cm, once the results for all mixed-layer depths have been collapsed on to one curve. The slope of the line is -1.17. (*b*) The entrainment relation obtained for a stroke of 3.22 cm, once the results for all mixed-layer depths have been collapsed on to one curve. The slope of the line is -1.23. Run NV2 was performed with $z_0 = 7.5$ cm, while the remaining three runs had $z_0 = 11.25$ cm.

exponent taking larger values than the mean for small Richardson numbers, and smaller values for large *Ri*.

This spread may be compared with the errors quoted by E & Hopfinger (1986). The value of n obtained from 3 runs with a stroke of 2 cm was 1.40 ± 0.15, and that from 3 runs with a stroke of 8.5 cm was 1.45 ± 0.05. The derivation of these error estimates is not explained in the paper, but certainly the spread seems similar to that obtained here.

Generally it has been assumed that the Reynolds number of the turbulence is

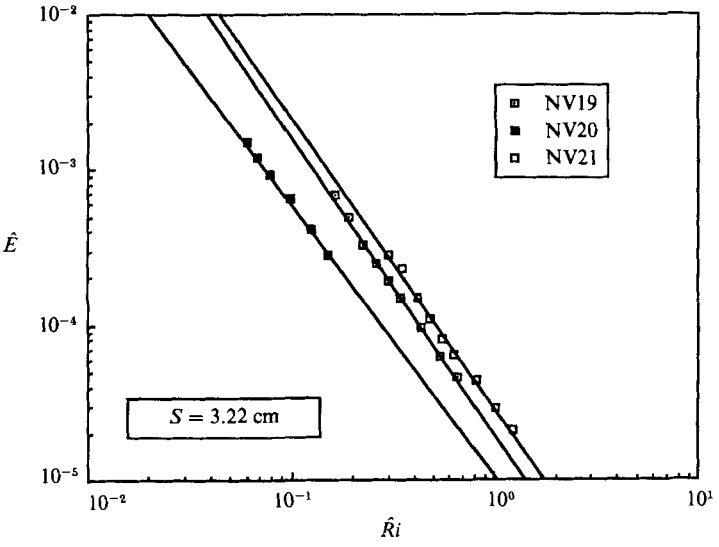

FIGURE 7. The results for runs NV19–NV21 re-analysed with a velocity decay of z^{-1}. The curves have slopes (from the left) of -1.81, -1.88 and -1.94.

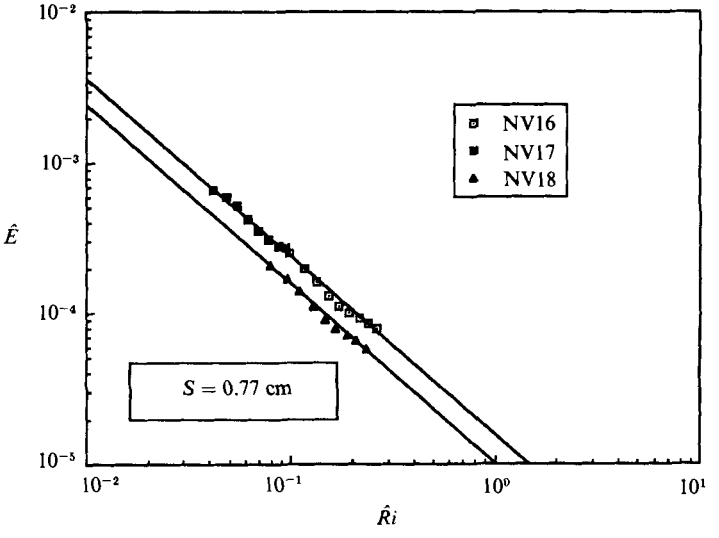

FIGURE 8. The results of runs NV16–NV18 demonstrate the effect of positioning the grid close to the bottom boundary. The grid was 3.84 cm from the tank bottom for runs NV16 and NV17. This distance was increased to 7.55 cm for run NV18, and the entrainment rate decreased for constant Ri.

constant, implying that the velocity decays like z^{-1}, provided that the turbulent lengthscale grows linearly with z. This decay is certainly significant different from that deduced from the results of this study. To illustrate the effect of an incorrect decay law the results for runs NV19–NV21 were replotted, assuming the velocity decayed like z^{-1}. The results are presented in figure 7. The power law exponents calculated from these curves are -1.94, -1.8 and -1.88, and the three curves can be seen to fall on distinct lines. We conclude that an incorrect decay law has a significant effect on the exponent deduced for the entrainment relation.

3.3. *The effect of a bottom boundary*

The distribution of turbulent kinetic energy in the flow is determined by the power input of the grid, the dissipation rate, the rate at which the potential energy of the system is increasing and the volume of water surrounding the grid. When the grid is placed close to the bottom boundary the volume of fluid is effectively reduced and the distribution of the turbulent energy will be affected. To test the importance of this the distance z_0 was varied for two strokes. The results for runs NV19–NV21 were analysed together, as z_0, the distance from the grid to the tank bottom, was 11.25 cm in all three cases. Using the deduced velocity decay law, the results of run NV2, for which $z_0 = 7.5$ cm, were analysed. As can be seen in figure 6(*b*), the results for NV2 lie on almost the same curve as the results for the other three runs. In this case the effect of the bottom boundary is insignificant. This result confirms that the bottom boundary has had no effect on the results for the two smaller strokes, $S = 1.6$ cm and $S = 2.4$ cm.

Runs NV16 and NV17 were both performed with the grid midplane 3.84 cm from the tank bottom. Z_0 was increased to 7.55 cm for run NV18 and it was found that the entrainment rates dropped somewhat (see figure 8). The presence of the bottom boundary has affected the intensity of the turbulent motions, but their rate of decay has remained essentially unchanged; a conclusion supported by the fact that the same velocity decay rate yields the same slope for the entrainment relation, even though z_0 has been altered.

In the experimental configurations of E & Hopfinger (1986) and Fernando & Long (1983, 1985) the grid was positioned in the top fluid layer, approximately 1 mesh size below the free surface. Although a free surface, with its ability to absorb energy as surface waves, will not affect the distribution of turbulent kinetic energy as much as a solid boundary, the effect of varying z_0 may still be important in these studies.

3.4. *The absolute entrainment law and the velocity dependence on stroke*

Unfortunately, absolute turbulent velocity measurements could not be made. The constant of proportionality in the relation between E and Ri, when these quantities are expressed in terms of the actual turbulent velocities, can be achieved only by resorting to the measurements of other experimenters and for this purpose the results of McDougall were used.

According to the results of Hopfinger & Toly (1976) β, the constant relating the turbulent lengthscale to the distance from the grid, increases approximately linearly with stroke. The results for strokes of 1.6 and 2.4 cm in the present study imply that the ratio l/u^2 is independent of stroke. If this is assumed to be valid for a stroke of 1 cm also (the stroke used in McDougall's experiments), by using Hopfinger & Toly's results for the increase of β with stroke the turbulent velocities measured by McDougall may be used to calibrate the present experiments for a stroke of 1.6 cm. A collapse of the results for the remaining strokes is then accomplished by translating the relative entrainment curves onto the absolute relation deduced for a 1.6 cm stroke. The resulting entrainment relation is plotted in figure 9. It is best expressed as

$$E = 0.15 Ri^{-1.21}. \tag{12}$$

The value for K of 0.15 is more than an order of magnitude less than that quoted by E & Hopfinger (1986), although it must be remembered that, in a power law relation of this kind, valid for Richardson numbers up to several hundred, the value of K depends strongly on the exponent. For instance, if the results from this study,

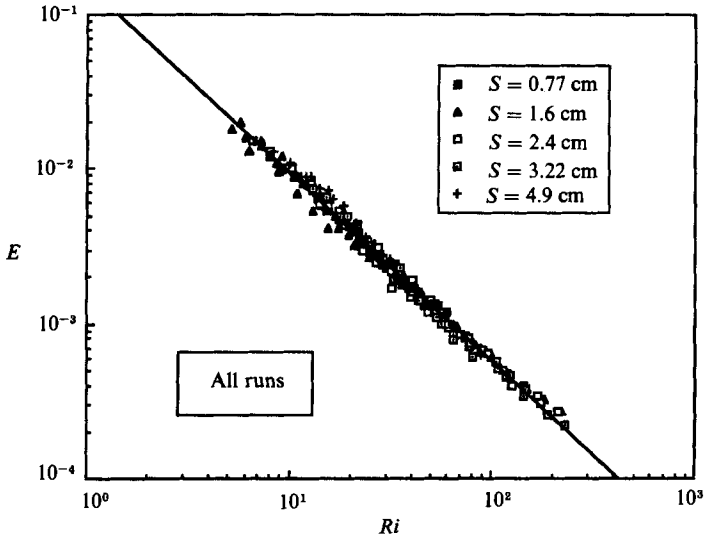

FIGURE 9. The results from all runs have been combined in this plot. McDougall's (1979) velocity measurements have transformed the entrainment rate, E, and Richardson number, Ri, to true values. The line corresponds to the function $E = 0.15Ri^{-1.21}$.

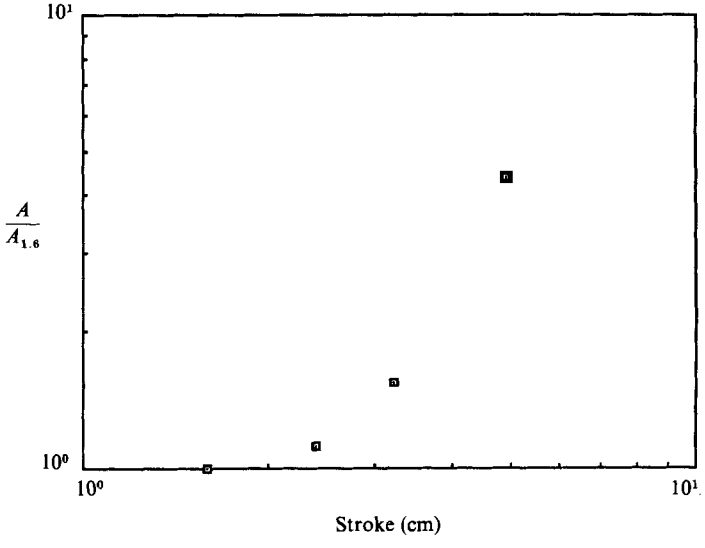

FIGURE 10. The dimensionless constant A, divided by the value for $S = 1.6$ cm, is plotted against stroke.

and those of E & Hopfinger's were assumed to coincide at $Ri = 50$ (a typical value for the range covered), the K-value associated with an exponent of -1.21 would need to be more than a factor of 3 less than that associated with an exponent of -1.5. Indeed, E & Hopfinger (1986) point out that the deduced value of K should not be given undue weight, because of the high power with which the velocity enters the expression for u_e (see §2). Turner's (1968) results, quoted in this book, Turner (1973), have been non-dimensionalized with Thompson's velocity measurements. Using these, instead of McDougall's, would double the value of K given in equation (12).

The stroke dependence of the turbulent velocity scale was deduced from this final

collapse of the entrainment relations for each stroke, by using the linear dependence of β on stroke, derived from the results of Hopfinger & Toly (1976). This dependence is contained in the non-dimensional constant A, defined in (7). This quantity, divided by its value for a stroke of 1.6 cm, is plotted against stroke in figure 10. As they stand the results demonstrate that the stroke dependence of the velocity cannot be represented by a simple power law.

4. Discussion

The results of this study have failed to verify the exponents in either of the power law entrainment relations proposed by Fernando & Long (1983, 1985) or E & Hopfinger (1986). However, it is in agreement with the suggestion of McDougall (1978). The results suggest a decrease in the non-dimensional entrainment velocity with increasing Richardson number of the form, $E \propto Ri^{-1.21}$. It is felt that these results have been obtained in the most consistent way, by analysing together the data obtained at a fixed distance from the grid. This precludes the necessity of employing an empirical relation for the velocity decay.

The sensitivity of the entrainment relation to the assumed form of the velocity decay has been stressed throughout this paper. An error in the magnitude of the velocity results in an incorrect estimate of the constant of proportionality, K, while an incorrect exponent in the velocity decay law causes a significant error in the deduced exponent of the entrainment relation. It is therefore risky to accept an empirical expression for the turbulent velocity, particularly if this expression has been obtained from measurements in a different experimental configuration to the one in which the mixing rates are being obtained. It should be noted also, that while Hopfinger & Toly (1976) quote a velocity decay of z^{-1} their results exhibited some spread. In particular, for a small stroke to mesh ratio they found the decay was closer to $z^{-1.25}$, at least up to 20 cm from the grid. This result was not used in the later paper of E & Hopfinger (1986) although a small stroke of 2 cm was used. This marginally different exponent in the velocity decay certainly would have decreased the magnitude of n.

It is the conclusion of this study that errors in the assumed form of the turbulent velocity scale may be the cause for the discrepancy between the entrainment relations deduced by different researchers. Furthermore, the errors associated with the exponent, n, are not negligible, and the uncertainties in determining this quantity are likely to be at least 10–15%.

I wish to thank Dr Greg Ivey for countless helpful discussions, and Professor Stewart Turner for his suggestions and comments. My gratitude is also extended to Mr Pat Travers who constructed the experimental equipment, and Messrs Ross Wylde-Browne and Derek Corrigan for their technical support. I also wish to thank two of the referees for their penetrating and constructive criticisms.

REFERENCES

Crapper, P. F. & Linden, P. F. 1974 The structure of turbulent density interfaces. *J. Fluid Mech.* **65**, 45–63.

Dickinson, S. C. & Long, R. R. 1978 Laboratory study of the growth of a turbulent layer of fluid. *Phys. Fluids* **21**, 1698–1701.

Dickinson, S. C. & Long, R. R. 1983 Oscillating-grid turbulence including effects of rotation. *J. Fluid Mech.* **126**, 315–333.

E, X. & HOPFINGER, E. J. 1986 On mixing across an interface in a stably stratified fluid. *J. Fluid Mech.* **166**, 227–244.

FERNANDO, H. J. S. & LONG, R. R. 1983 The growth of a grid-generated turbulent mixed layer in a two-fluid system. *J. Fluid Mech.* **133**, 377–395.

FERNANDO, H. J. S. & LONG, R. R. 1985 On the nature of the entrainment interface of a two-layer fluid subjected to zero-mean-shear turbulence. *J. Fluid Mech.* **151**, 21–53.

FOLSE, R. F., COX, T. P. & SCHEXNAYDER, K. R. 1981 Measurements of the growth of a turbulently mixed layer in a linearly stratified fluid. *Phys. Fluids* **24**, 396–400.

HANNOUN, I. A., FERNANDO, H. J. S. & LIST, E. J. 1988 Turbulence structure near a sharp density interface. *J. Fluid Mech.* **189**, 189–209.

HANNOUN, I. A. & LIST, E. J. 1988 Turbulent mixing at a shear-free density interface. *J. Fluid Mech.* **189**, 211–234.

HOPFINGER, E. J. & TOLY, J.-A. 1976 Spatially decaying turbulence and its relation to mixing across density interfaces. *J. Fluid Mech.* **78**, 155–175.

LINDEN, P. F. 1973 The interaction of a vortex ring with a sharp density interface: a model for turbulent entrainment. *J. Fluid Mech.* **60**, 467–480.

LINDEN, P. F. 1975 The deepening of a mixed layer in a stratified fluid. *J. Fluid Mech.* **71**, 385–405.

LONG, R. R. 1978 A theory of mixing in a stably stratified fluid. *J. Fluid Mech.* **84**, 113–124.

LONG, R. R. 1978 Theory of turbulence in a homogeneous fluid induced by an oscillating grid. *Phys. Fluids* **21**, 1887–1888.

MCDOUGALL, T. J. 1978 Some aspects of geophysical turbulence. Ph.D thesis, University of Cambridge.

MCDOUGALL, T. J. 1979 Measurements of turbulence in a zero-mean shear mixed layer. *J. Fluid Mech.* **94**, 409–431.

PHILLIPS, O. M. 1977 *Dynamics of the Upper Ocean.* Cambridge University Press.

ROUSE, H. & DODU, J. 1955 Turbulent diffusion across a density discontinuity. *Houille Blanche* **10**, 530–532.

THOMPSON, S. M. 1969 Turbulent interfaces generated by an oscillating grid in a stably stratified fluid. Ph.D thesis, University of Cambridge.

THOMPSON S. M. & TURNER, J. S. 1975 Mixing across an interface due to turbulence generated by an oscillating grid. *J. Fluid Mech.* **67**, 349–368.

TURNER, J. S. 1968 The influence of molecular diffusivity on turbulent entrainment across a density interface. *J. Fluid Mech.* **33**, 639–656.

TURNER, J. S. 1973 *Buoyancy Effects in Fluids.* Cambridge University Press.

WEAST, R. C. 1984 (ed.) *Handbook of Chemistry and Physics*, 65th edn. C.R.C. Press.

WOLANSKI, E. J. & BRUSH, L. M. 1975 Turbulent entrainment across stable density step structures. *Tellus* **27**, 259–268.